High-Efficiency Power Production from Coal with Carbon Capture

Thomas A. Adams II and Paul I. Barton
Dept. of Chemical Engineering, Massachusetts Institute of Technology, Cambridge, MA 02142

DOI 10.1002/aic.12230
Published online March 31, 2010 in Wiley Online Library (wileyonlinelibrary.com).

A zero-emissions power plant with high efficiency is presented. Syngas, produced by the gasification of coal, is shifted to produce H_2 which in turn fuels stacks of solid oxide fuel cells. Because the fuel cells maintain separate anode and cathode streams, air can be used as the oxygen source without diluting the fuel exhaust with nitrogen. This enables recovery of CO_2 from the exhaust with a very small energy penalty. As a result, an absorption-based CO_2 recovery process is avoided, as well as the production of large quantities of high-purity O_2, allowing a high overall thermal efficiency and essentially eliminating the energy penalty for carbon capture. © 2010 American Institute of Chemical Engineers *AIChE J,* 56: 3120–3136, 2010
Keywords: coal, power, solid oxide fuel cell, carbon capture, gasification

Introduction

Coal and CO_2

The implementation of federal regulations on CO_2 emissions in the United States is imminent, whether through simple emission restrictions or through a cap-and-trade system. This, combined with an increasing societal willingness to bear the costs of green energy, has prompted research and development of more environmentally friendly methods for producing electricity.

Coal with CO_2 capture is one such option that has prompted much debate and speculation. Currently, coal accounts for roughly one-third of all electricity production worldwide and is projected to account for 22% of all energy needs by 2030.[1] However, CO_2 generated as a byproduct of coal use accounts for about one-third of all CO_2 emissions arising from fossil fuels.[2] Therefore, new technologies aim to harness this abundant and low-cost resource while reducing the environmental consequences, receiving recent support from the US Secretary of Energy.[3] In particular, many new processes are being developed in which CO_2 is captured and then sequestered in a subterranean geological formation such as a saline aquifer, spent oil field, or other underground void space.[4] Typically, a goal of 90% carbon capture is sought.[5]

Combustion systems

Many CO_2-capture-enabled coal technologies rely on gasification, where coal is converted to syngas (a mixture of predominantly CO, CO_2, H_2, and H_2O) in a gasifier at high temperature and pressure, rather than directly burned as in traditional pulverized coal (PC) processes. During gasification, ''incombustibles'' are captured in a molten form called slag, rather than released as fly ash. Impurities in the syngas containing Hg, Cl, and S can be recovered in condensed form through various methods, yielding a fuel stream mostly free of regulated pollutants. The clean syngas can then be used for a variety of power production strategies with reduced CO_2 emissions.

In combination with the above syngas generation technique, the integrated gasification combined cycle (IGCC) approach converts the CO in the syngas to additional H_2 through the water gas shift (WGS) reaction. About 90% of the CO_2 can be removed from the shifted syngas at this point through solvent-based absorption, leaving a fuel stream consisting mostly of H_2. This H_2 is then combusted with air and expanded with a nitrogen diluent in a high-temperature gas turbine, generating electricity. The waste heat is recovered and converted to electricity in a steam bottoming cycle.

Additional Supporting Information may be found in the online version of this article.

Correspondence concerning this article should be addressed to P. I. Barton at pib@mit.edu.

The fuel exhaust consists primarily of water, nitrogen, and the unrecovered CO_2. Because the CO_2 is dilute, no further CO_2 capture is attempted and the exhaust is released to the atmosphere through the flue. Without carbon capture, IGCC processes are generally more efficient than their PC counterparts. Adding carbon capture and sequestration (CCS) capability, however, requires a significant energy penalty greater than the efficiency gains obtained by using gasification. Nevertheless, adding CCS to a traditional PC plant is even worse,[6] and so IGCC with CCS is currently seen as the most efficient low-emissions coal process feasible today.

Oxycombustion methods significantly reduce the energy penalty of the CO_2 recovery step by recovering CO_2 from the fuel exhaust stream, rather than through absorption.[7] Pure O_2 is used instead of air, leaving a fuel exhaust consisting primarily of water and CO_2, which requires significantly less energy to separate. However, the generation of a sufficient supply of high-purity O_2 through cryogenic air separation usually requires more power than that saved by avoiding absorption. Future techniques that may generate high-pressure O_2 more efficiently such as ionic transport membranes[8] and ceramic autothermal recovery[9] are promising, but have yet to be proven at large scales. In another approach, chemical looping can be used to provide oxygen to the fuel by means of a metal-oxide carrier.[10] Again, the resulting exhaust gases are primarily water and CO_2, from which spent solid metal particles are readily separated. However, the savings are offset by the costs of regenerating the carrier.

Solid oxide fuel cells

Solid oxide fuel cells (SOFCs) produce electricity from H_2 by an electrochemical reaction, rather than through combustion. Without the thermodynamic limitation of a heat engine, SOFCs achieve a higher electrical efficiency. For example, the gas turbine in an IGCC plant can be replaced by a SOFC unit, providing a higher plant efficiency.[11–17] However, as shown in this article, significant improvements can be made. SOFCs can be designed so that the anode (fuel side) and cathode (oxygen side) exhaust streams are not mixed, which can lead to some efficiency gains.[14] This allows the use of air as the oxygen source without diluting the fuel exhaust stream with nitrogen. Thus, the fuel exhaust consists essentially of CO_2 and H_2O, which can be separated through a flash cascade without the need for additional solvents. Thus, the upstream CO_2 absorption step can be avoided, further increasing the efficiency of the plant.

Recent developments in SOFC technology have been promising. For stationary power generation, companies such as Siemens, FuelCell and Energy, and Versa Power Systems have demonstrated stacks of SOFCs in the 10–30 kW range with a variety of fuels.[18,19] Future goals of the Solid State Energy Conversion Alliance (SECA) include the operation of 1 MW scale coal-based SOFC systems in 2012, 5 MW systems in 2015, and eventually industrial scale 250–500 MW plants by 2020.[20] In this article, we describe a novel process using this concept, showing how electricity can be generated from coal with CCS while maintaining a high efficiency, and assume that the ongoing scale-up of SOFC technology to industrial scales will be successful.

Process Model Description

The process to generate electricity from coal with zero emissions and 100% carbon capture is shown in Figure 1, with corresponding stream conditions in Table 1. Briefly, the process consists of nine steps: (1) air separation, where O_2 is produced, (2) gasification, where coal is converted to syngas using the O_2, (3) cleaning, where HCl is removed from the syngas, (4) shifting, where CO in the syngas is reacted with water to produce fuel rich in H_2 and CO_2, (5) fuel impurity removal, such as H_2S, NH_3, and Hg, (6) power generation, where the H_2 rich fuel powers SOFCs, (7) heat recovery, where steam is generated using waste heat from the SOFC exhausts and other areas of the plant, (8) CO_2 recovery, where the cooled fuel exhaust (chiefly H_2O and CO_2) is separated, and (9) CO_2 compression, where recovered CO_2 is cooled, compressed to supercritical pressures, and distributed in a pipeline. Each of these steps will be detailed in the proceeding sections.

For the calculations presented in this article, Illinois Bituminous #6 coal is supplied at a rate of 227 tonnes/h, with a HHV thermal input of 1711 MW, as received. By ultimate analysis, the coal contains 11.12 wt % moisture, 63.75 wt % C, 4.5 wt % H, 1.25 wt % N, 0.29 wt % Cl, 2.51 wt % S, and the balance ash. These conditions correspond to the IGCC with CCS process described in Woods et al.,[6] which is commonly cited as a baseline for comparison.

Simulations were performed in Aspen Plus 2006.5,[21] using the Peng-Robinson equation of state with the Boston-Mathias modification (PR-BM) for the flowsheet, with a few exceptions: (1) NBC/NRC steam tables were used for pure water streams, (2) streams consisting mostly of CO_2 and H_2O near the critical point were modeled using the Electrolyte-NRTL method with Henry coefficients and electrolyte chemistry specifications obtained from the AP065 databank, and (3) streams rich in CO_2 and H_2O away from the critical point were modeled with the Redlich-Kwong-Soave EOS with predictive Holderbaum mixing rules (the PSRK method). When compared against experimental data of CO_2/H_2O mixtures at vapor–liquid equilibrium for a wide range of temperatures and pressures,[22,23] it was found that the Electrolyte-NRTL and PSRK methods were far superior to other methods at accurately predicting both liquid and vapor phase solubilities, with the PSRK method slightly better overall. However, near the critical point, Aspen Plus could not find stable roots using the PSRK and other methods, and so the Electrolyte-NRTL model was used instead. One example is shown in Figure 2. The PR-BM model predicts phase properties more accurately for streams rich in components other than CO_2 and H_2O. For example, it was found that mixtures of CO_2 and N_2 near the critical point of CO_2 (69–74 bar) were best modeled with PR-BM when compared with experimental data.[24–26]

The following sections describe the models used for simulation in detail. The assumptions used throughout the simulation are summarized in Table 2.

Air separation

The air separation unit (ASU) collects air and recovers oxygen by cryogenic distillation. The oxygen is primarily used

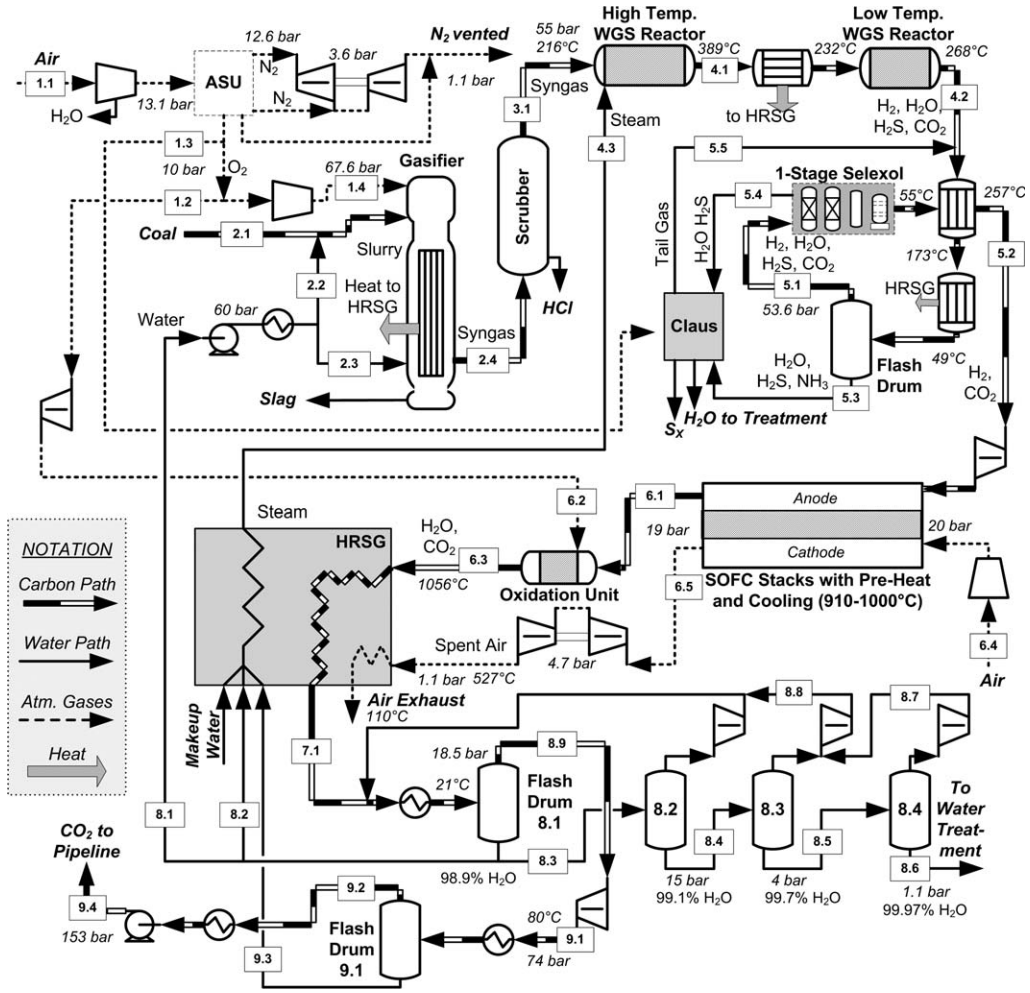

Figure 1. An integrated gasification—solid oxide fuel cell power plant.

in the gasifier, with a small amount used for oxidation in the power generation section and for the Claus process in the sulfur removal section. Air (stream 1.1) is first compressed to 13.1 bar with four stage compression, with water removed via interstage coolers operating at 31°C. The dehydrated air is sent to the cryogenic distillation unit, which is assumed to have the following separation conditions, based on those of Woods et al.[6]: Oxygen is recovered at 10 bar and 32.2°C with the fractional recoveries of O_2, N_2, and Ar being 0.94, 0.005, and 0.704, respectively; N_2 is recovered at 12.6 bar and 10°C with the fractional recoveries being 0.0023, 0.119, and 0.024, respectively; medium pressure N_2 is recovered at 3.9 bar and 32.2°C with fractional recoveries being 0.0147, 0.736, and 0.146, respectively; and the balance of the gases are lost to the atmosphere at 1.1 bar. In Aspen Plus, this is modeled by a specification block for simplicity. The nitrogen streams at pressure are expanded through turbines to recover power and then vented to the atmosphere.

The ASU used for this study was originally designed for an IGCC plant where pressurized nitrogen is needed for downstream processes, such as the main gas turbine. A detailed design of the ASU is underway at the MIT energy initiative. For this process, efficiency improvements may be possible by altering the design so that high pressure nitrogen is not produced in the first place, because it is not needed. This is an area of future study.

Although cryogenic separation is the most practical method currently available at very large scales, promising technologies such as ceramic autothermal recovery[9] and ionic transport membranes[8] may provide a better solution as those technologies are improved.

Gasification

In the gasifier, a slurry of coal and water is converted to syngas, a mixture of H_2, CO, H_2O, CO_2, and gaseous impurities such as N_2, Ar, HCl, H_2S, COS, NH_3, Hg, and CH_4. The water is provided by recycle from downstream units and may contain a small amount of CO_2 (<1%). Some of the heat from the gasifier is recovered to generate steam in the heat recovery and steam generation (HRSG) section of the plant. The remaining cooling is provided by quenching with additional water. Incombustible materials such as silicon dioxide, aluminum dioxide, calcium oxide, iron oxides, potassium oxide, and others[36] are collected in molten form as slag at the bottom of the gasifier, which can be cooled

Table 1. Stream Conditions Corresponding to Figure 1

Stream		1.1	1.2	1.3	1.4	2.1*	2.2	2.3	2.4	3.1	4.1	4.2	4.3
T (°C)		15	32	32	91	129	60	100	210	210	389	268	275
P (bar)		1.0	10.0	10.0	67.6	72.4	60.0	60.0	55.0	55.0	54.3	53.6	60.3
F (kmol/h)		29,597	86	96	5904	226,968	5228	6100	29,967	29,948	36,972	36,972	7024
Vapor frac.		1	1	1	1	Solid	0.01	0.01	1	1	1	1	0.93
Mole fractions	H_2O	1.1%				Illinois #6	99%	99%	31.6%	31.6%	26.7%	23.2%	99.6%
	O_2	20.8%	94.9%	94.9%	94.9%	Bituminous Coal	3 ppb	3 ppb					1 ppb
	N_2	77.2%	1.9%	1.9%	1.9%		3 ppm	3 ppm	0.7%	0.7%	0.6%	0.6%	1 ppm
	Ar	0.9%	3.2%	3.2%	3.2%		7 ppm	7 ppm	0.6%	0.6%	0.5%	0.5%	3 ppm
	CO								27.4%	27.4%	4.4%	0.9%	
	CO_2	300 ppm					1%	1%	12.2%	12.3%	27.8%	31.3%	0.4%
	H_2						10 ppb	10 ppb	26.7%	26.7%	39.4%	42.9%	4 ppb
	NH_3								40 ppm	40 ppm	32 ppm	32 ppm	
	COS								258 ppm	258 ppm	4 ppm	4 ppm	
	H_2S								0.6%	0.6%	0.5%	0.5%	446 ppb
	HCl								627 ppm				
	CH_4						7 ppb	7 ppb	694 ppm	694 ppm	562 ppm	562 ppm	3 ppb

Stream		5.1	5.2	5.3	5.4	5.5	6.1	6.2	6.3	6.4	6.5	7.1	8.1
T (°C)		49	257	49	49	353	1031	117	1168	15	1031	105	21
P (bar)		53.5	53.5	53.5	2.1	53.5	18.6	19.1	18.6	1.0	18.6	18.6	18.4
F (kmol/h)		28,686	28,212	8549	474	264	28,212	86	28,258	40,000	31,933	28,258	11,328
Vapor frac.		1	1	0	0.86	1	1	1	1	1	1	0.47	0
Mole fractions	H_2O	0.3%		99.3%	18.4%	0.2%	56%		56.3%	1.1%	1.4%	56.3%	99%
	O_2							94.9%	3 ppm	20.8%	0.7%	3 ppm	3 ppb
	N_2	0.8%	0.8%	4 ppm	6.1%	11%	0.8%	1.9%	0.8%	77.2%	96.7%	0.8%	3 ppm
	Ar	0.7%	0.7%	6 ppm		192 ppm	0.7%	3.2%	0.7%	0.9%	1.2%	0.7%	7 ppm
	CO	1.2%	1.2%	8 ppm		17 ppm	61 ppm		613 ppb			613 ppb	
	CO_2	41%	41%	0.6%	37.2%	85.7%	42.2%		42.3%	300 ppm	376 ppm	42.3%	1%
	H_2	55.3%	56.2%	387 ppm		0.2%	0.3%		28 ppm			28 ppm	10 ppb
	NH_3	3 ppb		140 ppm	168 ppb								
	COS	4 ppm		8 ppm	223 ppm	78 ppm							
	H_2S	0.6%	26 ppm	304 ppm	38.3%	2.9%	26 ppm		26 ppm			26 ppm	1 ppm
	CH_4	725 ppm	737 ppm	594 ppb		19 ppm	737 ppm		7 ppm		7 ppm	7 ppb	7 ppb

Stream		8.2	8.3	8.4	8.5	8.6	8.7	8.8	8.9	9.1	9.2	9.3	9.4
T (°C)		21	21	21	21	21	21	281	21	80	7†	7†	44
P (bar)		18.4	18.4	15.0	1.1	1.1	1.1	18.5	18.4	74.0	74.0	74.0	153.0
F (kmol/h)		2650	2071	2068	2052	2051	4	17	12,228	12,228	12,213	15	12,213
Vapor frac.		0	0	0	0	0	1	1	1	1	1	0	0
Mole fractions	H_2O	99%	99%	99.1%	99.9%	100%	2.2%	1%	0.2%	0.2%	501 ppm	95.4%	501 ppm
	O_2	3 ppb	3 ppb				4 ppb	70 ppb	6 ppm	6 ppm	6 ppm	20 ppb	6 ppm
	N_2	3 ppm	3 ppm	212 ppb			442 ppb	25 ppm	1.7%	1.7%	1.7%	30 ppm	1.7%
	Ar	7 ppm	7 ppm	1 ppm			8 ppm	146 ppm	1.6%	1.6%	1.6%	56 ppm	1.6%
	CO							9 ppb	1 ppm	1 ppm	1 ppm	3 ppb	1 ppm
	CO_2	1%	1%	0.9%	649 ppm	305 ppm	97.7%	98.9%	96.5%	96.5%	96.6%	4.6%	96.6%
	H_2	10 ppb	10 ppb				1 ppb	81 ppb	65 ppm	65 ppm	65 ppm	187 ppb	65 ppm
	H_2S	1 ppm	1 ppm	1 ppm	174 ppb	120 ppb	146 ppm	112 ppm	58 ppm	58 ppm	58 ppm	6 ppm	58 ppm
	CH_4	7 ppb	1 ppb			8 ppb	155 ppb	155 ppb	17 ppm	17 ppm	17 ppm	47 ppb	17 ppm

*Flow unit is kg/h.
†See the "CO_2 compression" section for explanation.

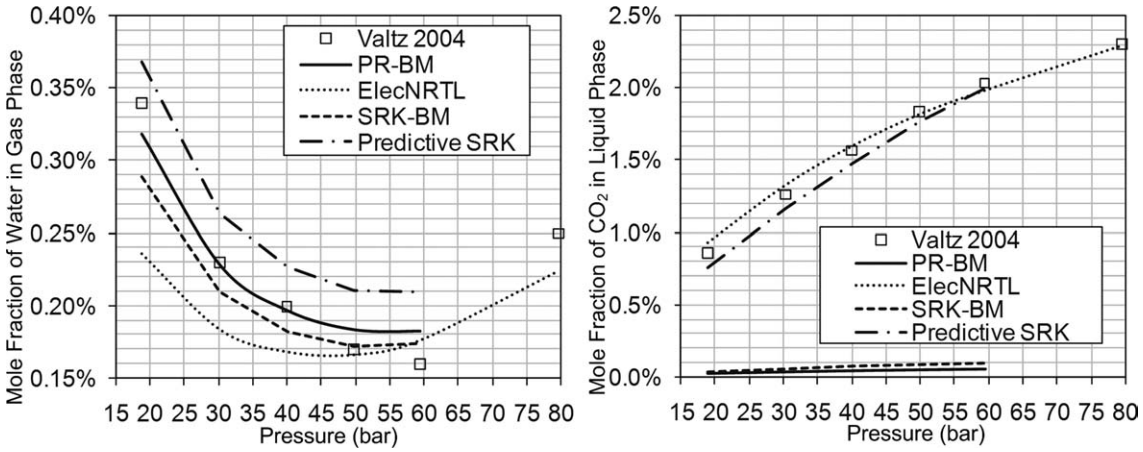

Figure 2. Predicted equilibrium solubilities of a mixture of CO_2 and H_2O at 308.2 K using: Peng-Robinson with Boston-Mathias (PR-BM), electrolyte-NRTL (ElecNRTL), Soave-Redlich-Kwong with Boston-Mathias (SRK-BM), and predictive Soave-Redlich-Kwong (Predictive SRK).

Data points (squares) are from Valtz et al.[22]

and used in other applications, such as road building materials.

To compare with the IGCC plant of Woods et al.,[6] the same gasifier specifications are used, namely, a GE Radiant-Only gasifier at 56 bar and 1300°C. Note that other commercially available gasifiers operate at different conditions and may produce syngas with different characteristics. The gasifier was modeled with three different steps: coal decomposition, gasification, and cooling. In the decomposition step, coal is broken down into solid C and S elements, as well as gaseous compounds such as H_2, H_2O, and Cl_2. The gasification step is modeled as an equilibrium reactor. Here, the decomposed mixture is combined with the necessary O_2 and H_2O and brought to chemical equilibrium through the following reactions:

$$C + 0.5\,O_2 \leftrightarrow CO \quad (1)$$

$$C + O_2 \leftrightarrow CO_2 \quad (2)$$

$$Cl_2 + H_2 \leftrightarrow 2HCl \quad (3)$$

$$N_2 + 3H_2 \leftrightarrow NH_3 \quad (4)$$

$$C + 2H_2 \leftrightarrow CH_4 \quad (5)$$

$$S + H_2 \leftrightarrow H_2S \quad (6)$$

$$CO + S \leftrightarrow COS \quad (7)$$

$$H_2O + CO \leftrightarrow CO_2 + H_2 \quad (8)$$

About 2.4% of the HHV of the fuel is assumed to be lost to the environment as waste heat in the gasifier section.[29] Two heaters in series are used to simulate the cooling section of the gasifier. First, radiant heat is recovered in the HRSG with a specified hot outlet temperature of 593°C. Then, water is mixed with the syngas to quench the stream further, producing steam and cooling to 210°C. Slag is assumed to be perfectly removed at this point. More detailed models for the gasifier are in development at the MIT Energy Initiative and will be discussed in future publications.

Gas cleaning

The presence of HCl in the fuel for a solid oxide fuel cell can degrade its performance. For example, a 50% loss in current density can occur when exposed to a feed contaminated by 160 ppm of HCl.[37] By contrast, the raw syngas leaving the gasifier contains roughly 600 ppm of HCl and so must be removed via scrubbing or some other technique. A detailed design of the scrubbing system is out of the scope of this work. For simplicity, syngas scrubbing is modeled as 100% removal of HCl.

Table 2. Assumptions Used in Simulation

		Refs.
Compressors and Turbines		
Isentropic efficiency	0.72	21
Mechanical efficiency	1	21
Maximum inlet/outlet pressure ratio	5.0	27
Maximum outlet/inlet pressure ratio	5.0	27
Pumps		
Efficiency, using Aspen default method	0.68–0.85	21
Steam plant		
Max steam cycle temperature	550°C	28
Max steam cycle pressure	127 bar	28
Stage 2 pressure	28.2 bar	
Stage 3 pressure	6.3 bar	
Stage 4 pressure	1.4 bar	
Stage 5 pressure	0.4 bar	
Min steam cycle pressure	0.07 bar	6
Heat exchangers		
Minimum approach temperature	5°C	
Gasifier		
Gasifier heat losses	2.40%	29
Solid oxide fuel cells		
Fraction of free energy lost to environs	0.05	30
Overall fuel utilization	0.995	
Fuel cell voltage achieved	0.69 V	30–34
Maximum theoretical voltage	0.96 V	35
DC to AC conversion efficiency	0.96	31,35

Syngas shifting

Recently, it has been shown that SOFC fuels containing CO can cause power loss and degradation of the anode due to carbon deposition via the Boudouard reaction[38,39]:

$$2CO(g) \leftrightarrow CO_2(g) + C(s) \quad (9)$$

Chemical equilibrium predictions show the formation of a stable, graphitic carbon phase when CO is present in the SOFC anode under normal operating conditions.[40] This is also true for a range of fossil–fuel-derived syngas mixtures. Although Lim et al.[41] were able to run a SOFC for a month on a syngas fuel, the effects of long-term exposure on the usable lifetime are still unclear. Furthermore, the authors showed that more power was produced significantly when running the fuel cell on H_2 rather than a mixture of H_2 and CO, highlighting the negative impact of CO.

Thus, the WGS reaction, shown in Eq. 8, is used to convert the energy-bearing CO in the syngas to H_2. Although many variations are possible, two reactors in series are used: a high-temperature (300–450°C) packed-bed reactor and a low-temperature (200–300°C) packed-bed reactor, with an intermediate cooler. It is assumed that 80% conversion is achieved in the high temperature reactor, and the low temperature reaction approaches equilibrium, or about 96% conversion overall. More detailed models of the WGS reactors are currently under development by the authors.[42]

Additional steam, generated in the HRSG, must be added to the first reactor to bring the H_2O:CO ratio up to 2:1. Higher steam ratios will allow for a higher conversion but at the expense of increased equipment cost and fuel dilution. The reactor effluent consists of about 42 mol % H_2, with the balance mostly H_2O and CO_2 (the SOFC anode is tolerant of both). A pressure drop of 0.7 bar is assumed for each reactor.

Additionally, the COS hydrolysis reaction occurs in the WGS reactors:

$$COS + H_2O \leftrightarrow CO_2 + H_2S \quad (10)$$

Because of the very large H_2O:COS ratio, it is assumed that the COS achieves 100% conversion in the first WGS reactor. This is beneficial for sulfur recovery because H_2S can be more easily recovered from the fuel stream.

In practice, both reactors are packed with catalysts suitable for the operating temperature range. Typically, iron-based catalysts are used for the high-temperature reaction and copper-based catalysts are used at low temperatures.[43] Because H_2S remains in the syngas, both catalysts must be sulfur-tolerant, and many commercially available catalysts are suitable for this purpose. In fact, these ''sour shift'' catalysts may require a minimum sulfur concentration of 100 ppm or higher to prevent methanation and maximize their effectiveness, such as the cobalt-molybdenum catalyst C25-1-02 by Süd-Chemie.[44] If desired, the sulfur removal step (see next section) can take place upstream of the shift reactors so that a sulfur-sensitive catalyst may be used. These ''sweet-shift'' catalysts may require very good sulfur removal, as they may become damaged with as little as 100 ppm sulfur for high temperature catalysts and 0.1 ppm for low temperature catalysts.[45,46] For further discussion on the tradeoffs of sweet vs. sour WGS units in this context, see Grol and Yang.[46]

Impurity removal

Impurities such as sulfur, ammonia, and mercury are removed from the fuel gas before use in the SOFCs. Although SOFC anodes can tolerate a certain amount of ammonia,[35] it is most efficient to remove it before the Selexol process, since the feed to the first stage of that process must be cooled to near-ambient temperature anyway. Therefore, the shifted syngas (stream 4.2) is cooled to 49°C through a series of heat exchangers, condensing most of the water contained in the syngas. The liquid stream, containing most of the NH_3, is sent to the Claus process for treatment. The vapor stream is fed to a mercury removal unit (not shown in Figure 1). In this simulation, Hg was not considered and so this unit was not modeled in Aspen Plus.

Because SOFCs cannot tolerate concentrations of H_2S above 100 ppm,[31–33,39] the sulfur compounds must be removed before use in the power island. The syngas, now cleaned of NH_3 and Hg, is fed to a 1-Stage Selexol process. In this process, the syngas is contacted with liquid solvent (Selexol) at a Selexol:syngas molar ratio of roughly 0.2:1 in an absorption column. Most of the H_2S is recovered in the solvent (as well as a small amount of CO_2) leaving only about 25 ppm H_2S in the vapor product. The solvent is regenerated through a stripping process and reused. The H_2S and CO_2 released from the solvent are sent to the Claus process.

For simplicity, a specification block is used to simulate the 1-Stage Selexol process, which assumes that all of the H_2O, 99.6% of the H_2S, 12% of the N_2, 1.5% of the CO_2, and 100% of the COS are recovered in the sulfur stream sent to the Claus process (stream 5.4). These recoveries are based on the results of a more rigorous model currently in development at the MIT Energy Initiative, which will be described in future publications.

Oxygen generated in the ASU is combined with the H_2S gas stream and burned in the Claus furnace, producing sulfur compounds (S_X). The S_X are condensed from the gas stream through a variety of steps. Some unconverted H_2S remains, which is recycled to the 1-Stage Selexol process in the tail gas (stream 5.5). The Claus process was modeled using specified fractional recoveries representing the results of a more detailed model in development at MIT, based on that of Woods et al.[6] It is specified that 6.7% of CO, 98% of CO_2, 12.4% of H_2, 11.7% of COS, and 4.2% of H_2S in the total feed to the Claus process remains unrecovered in the tail gas.

It should be noted that other technologies for removing these impurities can be considered. For example, other solvents such as Rectisol, Sulfinol, Purisol, Flexsorb, and methyldiethanolamine are in active use for similar applications. We have chosen Selexol for consistency with the IGCC base case Woods et al.[6] Unfortunately, the use of these solvents typically requires near-ambient temperatures, which introduces a significant efficiency loss. To counter this, warm and hot syngas cleanup technologies are currently in development, such as the use of various sorbents to remove H_2S, HCl, and other impurities.[47] However, many technological

challenges remain, particularly when the treated fuel gas is destined for use in SOFCs.[48]

Power island

SOFCs provide the bulk of the power generated by the plant. Individual fuel cells are small, but many of them can be combined to create compartmentalized fuel cell modules. Each module can be arranged as needed (in parallel or series) based on certain design conditions. Because of the limits imposed by materials of construction, SOFCs typically operate at a maximum of roughly 1000°C and 20 bar. Higher temperatures and pressures generally achieve higher plant efficiencies,[35] but exceeding these limits can cause a failure of the seal between the anode and cathode, allowing the exhaust streams to mix and potentially destroying the functionality of the cell. Therefore, fuel cell modules are arranged in series with intermediate cooling stages to ensure that the temperature of the cell does not exceed the upper bound (assumed to be 1030°C for this example).

The cleaned syngas is first expanded to 20 bar, preheated to 910°C, and fed to the SOFC anode side. Likewise, ambient air is compressed and preheated to the same conditions, and fed to the cathode side. For many configurations, a sufficient amount of heat is available from interstage cooling to provide for the preheating needs. Otherwise, heat from other sources, such as the oxidation unit exhaust, can be used.

In the fuel cells, power is generated through the following reactions, noting that the CO in the feed will be in small quantities:

$$H_2 + O^{=} \rightarrow H_2O + 2e^{-} \quad \text{(anode)} \tag{11}$$

$$CO + O^{=} \rightarrow CO_2 + 2e^{-} \quad \text{(anode)} \tag{12}$$

$$O_2 + 4e^{-} \rightarrow 2O^{=} \quad \text{(cathode)} \tag{13}$$

Oxygen at the cathode encounters free electrons, producing ions ($O^{=}$). The ions travel through the solid electrolyte separating the anode and cathode via solid ionic conduction, not diffusion. Arriving at the anode, the oxygen ions then react with the fuel sources, oxidizing them and releasing electrons and heat. The electrons travel through the circuit, generating power from the free energy difference between cathode and anode.

In Aspen Plus, each module was simulated as shown in Figure 3. The anode and cathode inlets are first cooled to 910°C (or preheated for the first stage) and then mixed. The mixed stream then enters an isothermal reactor at 910°C with a specified 0.1 bar pressure drop. The conversion of H_2 and CO in the fuel cell module is set as the specified overall fuel conversion divided by the number of modules. For the stream conditions in Table 1, seven fuel cell modules are used in series with a specified total conversion of 99.5%, giving a conversion of ~2250 kmol/h of H_2 in each module. The effects of variations in these assumptions are described in the "Impact of model parameters" section.

The exothermic heat of reaction (ΔH) as calculated by Aspen in the reactor block represents the total energy change of the electrochemical reaction. The portion of that energy released as DC electricity ($W_{\text{module,DC}}$) is:

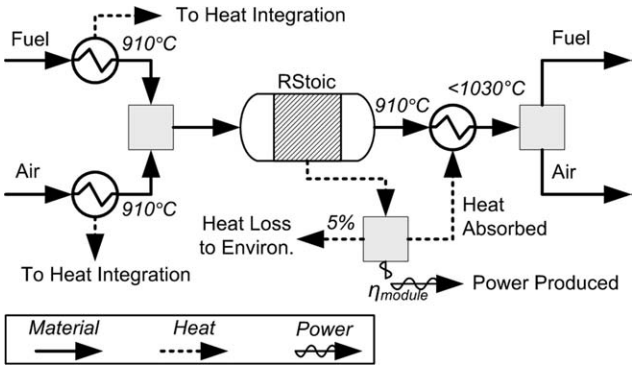

Figure 3. Aspen model used to simulate an individual SOFC module.

The fuel and air streams are combined to facilitate energy calculations, and are split again into their appropriate components by a calculator block.

$$W_{\text{module,DC}} = \eta_{\text{act}}(\Delta H - (1183.15K)\Delta S) \tag{14}$$

where ΔH and ΔS are the change in enthalpy and entropy, respectively, on reaction of the theoretically mixed anode and cathode streams, and η_{act} is the ratio of the actual voltage of the cell to the ideal voltage. The value for η_{act} (0.719) and its impact on the model is discussed in the "Impact of model parameters" section. Thus, the electrical efficiency of the fuel cell module (η_{module}) is:

$$\eta_{\text{module}} = W_{\text{module,DC}}/\Delta H \tag{15}$$

For many power distribution systems, it is necessary to convert DC power to AC. It is assumed that DC → AC inversion is 96% efficient,[31,35] giving an actual AC power production of:

$$W_{\text{module,AC}} = 0.96\, W_{\text{module,DC}} \tag{16}$$

It is also assumed that 5% of the free energy of reaction is lost to the environment as radiant waste heat.[30] Although few theoretical models consider environmental heat losses, some loss will inevitably occur at the high temperatures of the fuel cells, as it does in other high temperature unit operations. We note that our estimate may be somewhat conservative.

The remaining energy goes into heating the gas streams. In the model, this is simulated with a heater block for the theoretically mixed anode and cathode streams. Then, a separation block splits the mixed stream into the actual anode and cathode outputs. The calculated heat duties from all of the precoolers in the SOFC modules are combined and mixed to simulate heat integration of the preheater with the intermediate coolers. Excess heat is integrated with the HRSG for steam generation.

The spent air is expanded through multistage turbines to recover additional energy, providing for about 75% of the power required to compress the air to SOFC conditions. The expanded air still contains useful heat and is sent to the HRSG. The spent fuel contains small amounts of unreacted H_2, CO, and CH_4, and so this is fed to the adiabatic

oxidation unit where it is reacted with a stoichiometric amount of O_2 from the ASU. This produces more waste gases (H_2O and CO_2) and heat. Heat is recovered from the fuel exhaust in the HRSG.

HRSG

The heat recovery and steam generation section of the plant collects waste heat from across the plant to generate steam. Steam for the WGS unit is generated from a portion of the water condensate from the first CO_2/H_2O separation flash drum 8.1 mixed with the water condensate recovered from the final water removal drum 9.1. The remaining heat is used to generate steam in a bottoming steam cycle, with stage conditions listed in Table 2. The major heat sources are the cathode and anode exhausts, the WGS interstage cooler, the radiant heat from the gasifier, and the syngas cooler for NH_3 recovery. Because the design of an optimized heat exchanger network is out of the scope of this work, it is assumed that all heat available above 105°C can be recovered somewhere in the cycle. The bottoming cycle produces roughly 30% of the gross power for the plant.

CO_2 recovery

After cooling in the HRSG, the spent fuel consists primarily of H_2O and CO_2 at about 18.5 bar. This can be separated efficiently using a series of cascading flash drums.[49] The fuel exhaust is first cooled to 21°C and flashed in Drum 8.1. About 98.6% of the CO_2 in the feed to the drum is recovered in the vapor product. The liquid phase contains most of the water and the rest of the CO_2. A portion of this is recycled for the gasifier quench, coal slurry, or for the WGS reaction. The remaining water is further depressurized and separated in additional flash drums, recycling the vapor products to the first drum, permitting nearly 100% CO_2 capture overall. The final liquid product at atmospheric pressure contains 99.97% water.

The number and operating conditions of the flash drums are subject to further optimization. At least one high pressure and one atmospheric pressure drum are recommended. With only one flash stage, a high pressure flash (i.e., 18.5 bar) will only achieve about 98.6% CO_2 recovery, whereas a low pressure flash (i.e., 1.0 bar) will achieve about 100% capture but requires an additional 45 MW for additional pressurization of CO_2 and recycle water.

CO_2 compression

The CO_2 stream recovered from Flash Drum 8.1 is compressed to about 74 bar (just below the critical point) with two stage compression, cooled, and then flashed in Drum 9.1. The majority of the water remaining in the feed stream is recovered in the liquid phase and recycled for steam generation. The dehydrated CO_2 vapor stream is then totally condensed and pumped to supercritical pressure (153 bar) for distribution in the CO_2 pipeline. The CO_2 is recovered at a sufficiently high purity (>96%) with low enough water (500 ppm) and sulfur (58 ppm) contents to satisfy most existing CO_2 pipeline constraints.[50]

The Electrolyte-NRTL model was used for Flash Drum 9.1 because of the convergence issues discussed previously. Although the model predicts the gas and liquid concentrations well, the calculated temperature at which sufficient phase separation takes place (7°C) seems inaccurate. For example, the PSRK and PR-BM models (which are generally more accurate without water present) predict that the bubble point of dehydrated CO_2 stream 9.2 is 24–25°C. The appropriate temperature for this drum is somewhere above 26°C.

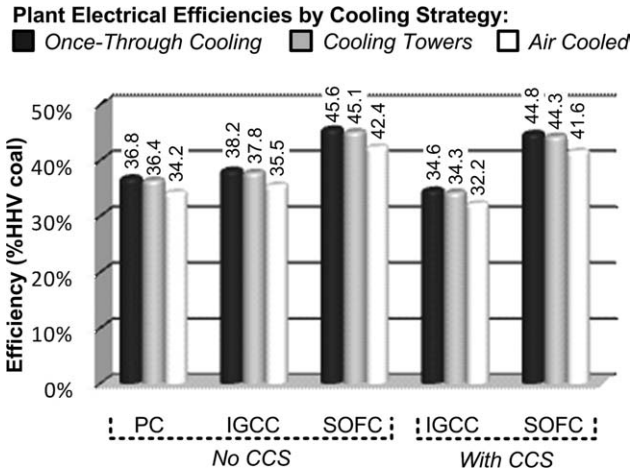

Figure 4. Comparison of power plant efficiencies (% HHV coal), for PC, IGCC, and the plant proposed in this article (SOFC), with or without CCS.

Results and Discussion

The SOFC-based power plant as a whole is significantly more efficient than the IGCC base case or traditional pulverized coal plants, even with CO_2 capture capability, as shown in Figure 4. The SOFC-based power plant with cooling towers achieves about 44.8% efficiency, which is significantly higher than IGCC at 38.2%, and typical pulverized coal at 36.8%. When CCS capability is included, the SOFC plant efficiency is reduced by less than 1 percentage-point (pp). However, the inclusion of CCS causes the IGCC plant to drop by about 6 pp and as much as 12 pp for PC. Although efficiencies may vary with the gasifier, turbine, and fuel choice, the general trend is the same.

Furthermore, though the efficiency boost comes at a larger capital expense, the levelized cost of electricity (LCOE) for the SOFC plant is 10–20% lower than the IGCC with CCS case, even with the conservative fuel cell cost estimate of $1000/kW. When compared with traditional pulverized coal without CCS, implementing the proposed SOFC with CCS technology would increase the LCOE to the consumer by 10–22%, significantly lower than the 30–40% increase predicted for IGCC and over 80% increase for pulverized coal. Thus, the SOFC process appears to be the most economical way of producing electricity from coal with carbon capture.

In addition to the efficiency and economic advantages, the SOFC process has significant environmental advantages as well. As a zero-emissions process, not only 100% of the CO_2 is captured and sequestered, but any other pollutants (SO_X, NO_X, etc.) are also sequestered in the pipeline. Additionally, more than enough water is recaptured (which would otherwise be vented to the atmosphere) to completely supply

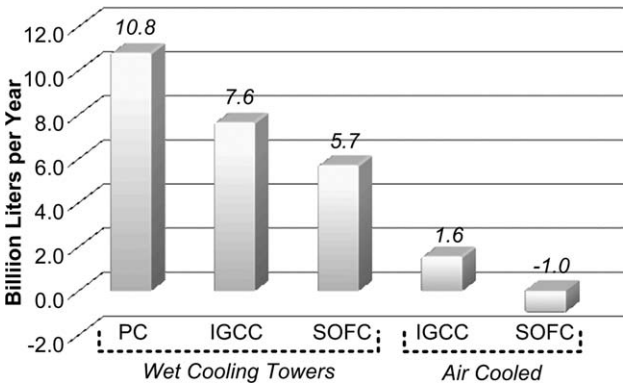

Figure 5. Water consumption for pulverized coal (PC), IGCC, and the plant proposed in this article (SOFC).

Carbon capture is considered in these cases except for PC.

the water consumption needs of the plant. Depending on the type of cooling system used, the plant would actually produce water, rather than consume it, as shown in Figure 5.

An in-depth discussion of the results can be found in the following subsections.

Impact of SOFC model parameters

The impact of assumptions used in modeling the SOFCs is explored in this section. In Figure 6A, the assumed ratio of the operating voltage to the ideal voltage (η_{act}) is varied from 62.5% to 100%, which at 910°C corresponds to an average achieved voltage range of 0.60–0.96 V. Note that the actual voltage achieved in each module will vary; large voltages may be achievable in the beginning modules where fuel concentration is high, and conversely the later modules with lower fuel concentrations may not be able to reach 0.6 V. A reasonable average achievable voltage for a variety of fuels with current and expected future technologies is about 0.6–0.8 V.[30–34] In practice, voltages will never reach the ideal maximums (0.96 V in this case) but are provided here to show the upper bound on the efficiency gains that can be made possible by improvements to SOFC technology.

As expected, the net power plant efficiency increases linearly with η_{act}, at a rate of 0.31 pp per 1 pp increase in η_{act}. This includes a 7.78 MW/pp increase in the SOFC output and a corresponding −2.50 MW/pp decrease in the power output of the HRSG due to the reduced amount of waste heat produced by the fuel cells. These large variations reflect the importance of the fuel cell efficiency, and suggest that as fuel cell technology improves and voltages closer to the ideal become attainable, significant improvements to the bottom line efficiency of the plant can be achieved.

The effect of fuel utilization, or the percent conversion of H_2 in the SOFC, is shown in Figure 6B. In this example, the specified fuel utilization of the fuel cells is varied while holding the amount of air in the cathode constant (with a 2:1 H_2 to O_2 ratio). The O_2 fed to the oxidation unit is adjusted so that the ratio of H_2 in stream 6.1 to O_2 in stream 6.2 is also stoichiometric (2:1). The effect of fuel utilization was also significant (though not as much as the effect of

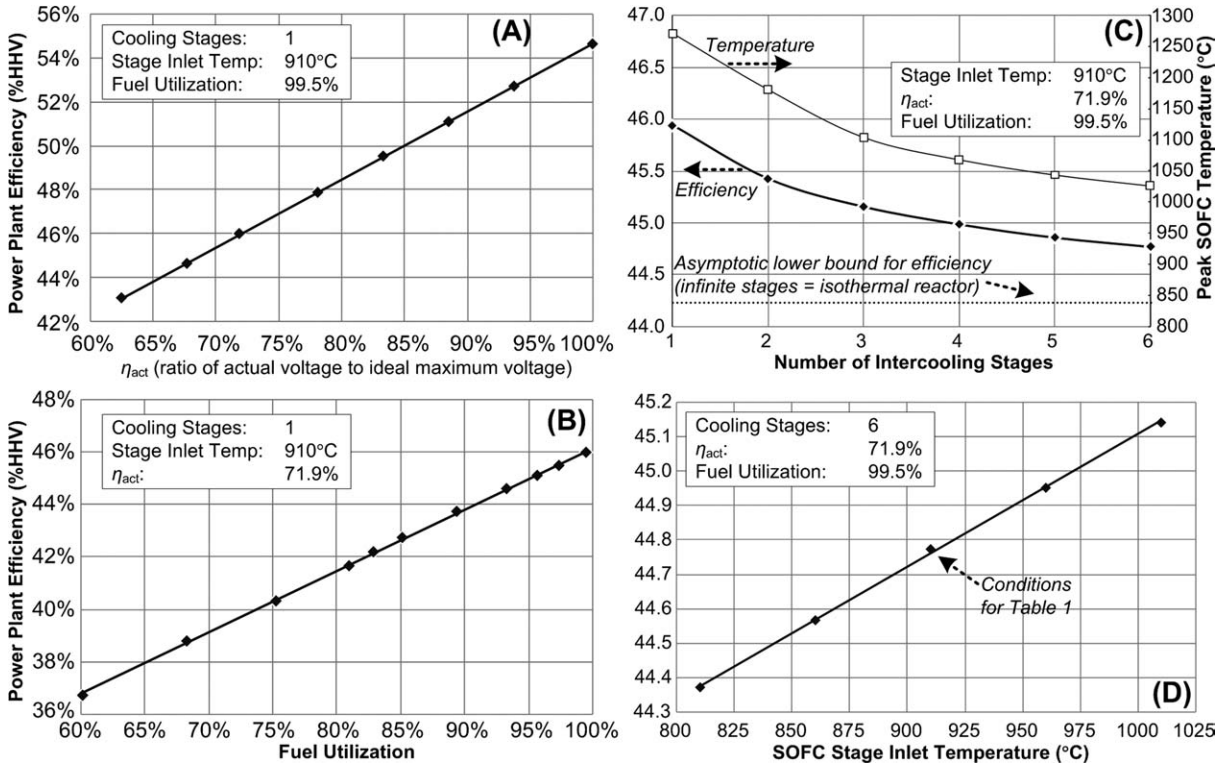

Figure 6. The effect of SOFC parameters on the power plant thermal efficiency.

(A), η_{act} and (B) Fuel utilization, a.k.a. percent conversion of the H_2 fuel. (C) The number of intercooling stages between fuel cell modules, and the resulting maximum SOFC temperature of the system. (D) The inlet temperature to each SOFC stage.

operating voltage), with an overall impact on the efficiency of about 0.23 pp per 1 pp increase in the fuel utilization, or about 4 MW/pp. Although the combined power output from the SOFC and steam plant increase at a rate of about 3.1 MW/pp in fuel utilization, the load on the ASU to provide the additional O_2 to the oxidization unit also decreases by 0.9 MW/pp.

The number of intercooling stages has a less significant effect. As shown in Figure 6C, as the number of intercooling stages are increased (that is, one less than the number of SOFC modules), the total plant efficiency drops asymptotically, with a maximum loss less than 2 pp. The maximum SOFC temperature is plotted on the right-hand axis, which decreases in a similar fashion to the asymptotic lower bound of the inlet temperature (910°C). To maximize efficiency, the minimum number of stages should be chosen such that the operating temperature of the SOFCs never exceeds their design upper bound, although having too many stages will not significantly penalize the efficiency. This is largely due to the small efficiency increase in the Brayton cycle that arises from higher temperatures, as shown in Figure 6D. Here, the inlet temperature to each SOFC module (using 6 intercooling stages) was varied over a 200°C range, resulting in only a 0.8 pp increase over that range.

The stream conditions in Table 1 and the results discussed in the following sections assume six intercooling stages, $\eta_{act} = 71.9\%$ (an average operating voltage over the seven modules of about 0.69 V), 99.5% fuel utilization, and module inlet temperatures of 910°C. The assumption for η_{act} is conservative, since recent studies with H_2 fuels (not containing CO) have measured higher voltages than 0.69 V at similar temperatures.[32,34] However, the low value of η_{act} attempts to account for the negative impact of trace H_2S remaining in the fuel feed, as well as the negative impact of the high fuel utilization.[35] Single-pass fuel utilizations of 85% have been technologically achievable for over a decade,[31] and anode recycle streams enable higher values.[51] Given ongoing technological improvements, the assumed value of 99.5% may not be overly optimistic by the time such a power plant would be constructed. This contribution to the overall plant efficiency is not likely to be overstated by more than 1–2 pp.

Table 3. Summary of Power Production in MW (Consumption is Negative) for the Proposed SOFC Process and the Baseline IGCC Process

Block	Unit	SOFC	IGCC
1	Air compression	−73.4	−72.4
	O_2 compression	−11.4	−11.4
	N_2 compression	–	−35.8
	High press N_2 turb.	1.3	–
	Med. press N_2 turb.	10.2	–
	Subtotal	*−73.4*	*−119.5*
2	Total pumps	−0.4	–
5	CO_2 separation	–	−13.6
	Total pumps	−4.3	−4.5
	Subtotal	*−4.3*	*−18.1*
6	SOFC stacks	563.0	–
	Gas turbine	–	836.2
	Spent air turb 1	81.1	–
	Spent air turb 2	66.4	–
	Fuel gas turbine	20.7	6.5
	Air compression	−186.9	−370.9
	O_2 compression	−0.1	–
	Subtotal	*544.2*	*471.9*
7	Steam turb 1	91.9	37.3
	Steam turb 2	73.1	26.1
	Steam turb 3	58.3	29.7
	Steam turb 4	41.3	61.6
	Steam turb 5	50.3	129.4
	Steam turb 6	3.8	
	Total pumps	−5.0	−5.3
	Subtotal	*313.7*	*278.7*
8	Total compress.	−0.1	–
9	Gas compression	−12.0	−18.4
	CO_2 pump	−1.7	−2.5
	Subtotal	*−13.8*	*−20.8*
10	Total pumps	−0.4	−0.4
Gross production		1061	1127
Gross consumption		296	535
Net production		766	592

Each process achieves >90% CO_2 capture and assumes once-through cooling with 227 tonne/h Illinois bituminous #6 coal feed.

Impact of air compression

One of the biggest parasitic power loads on gasification-based plants is the ASU, as shown in Table 3. This load arises from the high power requirement necessary to compress ambient air to ASU pressures before separation, and to further compress the recovered O_2 and N_2 streams to high pressure for use in the gasifier or gas turbine. Another major power load is the air compression step required in the power island to provide oxygen and/or nitrogen to the power generating machinery. For the IGCC example, these air compression loads combine to about 490 MW, or about 44% of the gross power output.

By replacing the gas turbine with a SOFC, the demand for high pressure air is significantly reduced. First, since the SOFC does not need to be diluted with N_2, the N_2 recovered from the ASU does not need to be compressed to high pressure. Instead, some power can be recovered through expansion turbines, saving a total of about 46 MW. Likewise, the air compressed and fed to the gas turbine for additional N_2 dilution can be reduced, saving about 184 MW. Together, this represents about 230 MW of savings, or about 20% of the gross power produced.

It should be noted that other dilution materials for the gas turbine in IGCC may be selected instead of N_2 (such as steam or CO_2), and that this decision will affect the greater flowsheet. For the IGCC case, the use of N_2 makes sense because a supply at medium pressure is already available from the ASU,[6] and additional air can provide for the remaining N_2 needs while also providing an oxygen source. This creates a large excess of oxygen in the combustor, which helps provide for complete combustion of the fuel. To contrast, the SOFC system uses a stoichiometric amount of oxygen in the SOFC anode, and thus the air compression load is significantly reduced. Other designs may use a surplus of oxygen in the

anode to improve the SOFC efficiency, but this will require a subsequent penalty to compress the additional air.

CO_2 capture consequences

For the IGCC case, the energy penalty of adding CO_2 capture capability to the process is about 4–6 pp. This arises partly from the 2-Stage Selexol process, where CO_2 is recovered upstream of the combustion turbines through absorption. As opposed to the 1-Stage Selexol process used with the SOFC-based plant, the 2-Stage version recovers both H_2S and CO_2 with the solvent Selexol. In the first stage, H_2S is removed from shifted syngas using a sequence of absorbers and strippers analogous to those described in the "Impurity removal" section. The desulfurized shifted syngas is sent to a second stage of absorbers and contacted with a large amount of Selexol. About 90% of the CO_2 is absorbed by the Selexol, and the CO_2-depleted fuel gas is sent to the power island. The loaded solvent is flashed at lower pressures, releasing the CO_2 (to be sent to the CO_2 pipeline) and regenerating the solvent. Based on the results of an ongoing study at MIT, the CO_2 recovery stage requires about 10 times the circulation rate of Selexol than does the H_2S recovery stage. As shown in Table 3, this requires about 14 MW of additional power, mostly for solvent pumping.

Removing CO_2 from the fuel gas has additional consequences, because CO_2 in the fuel also acts as a diluent in the gas turbine. Thus, additional nitrogen is needed to replace the CO_2, causing roughly a 17 MW increase in power consumption in the air and nitrogen compressors in the ASU.[6] Also, the capital cost of the CO_2 absorption stage (roughly 6% of the plant capital cost) is more than double that of the H_2S absorption stage (Bashadi S. MIT Energy Initiative, personal communication). With the SOFC design, the second Selexol stage is unnecessary, saving a significant amount of capital. Instead, the multistage flash unit handles CO_2 recovery for less than 0.1 MW power consumption. Furthermore, the capital cost of the flash-based CO_2 recovery process is about an order of magnitude less than the second Selexol stage, considering the significantly reduced complexity of equipment and the order of magnitude reduction in solvent usage.

Depending on the configuration, the cost of compressing the CO_2 to supercritical conditions once it is captured is roughly 14–27 MW (about 1–1.5 pp). This penalty varies depending on the purity of CO_2 recovered, the efficiency of the compressors, and the pressure at which CO_2 is captured. For most power plant configurations, this portion of the parasitic power load is unavoidable. Thus, the SOFC-based plant configuration essentially reduces the energy penalty for CO_2 capture down to the cost of compression.

Power island efficiency

It is worth noting that as the net power produced by the power island is greater for the SOFC case than for the IGCC, the gross output is not, as shown in Table 3. The IGCC gas turbine produces 836 MW of power and the SOFC stacks only produce 563 MW. This is because of the significantly larger mass flow rate through the gas turbine due to the addition of the diluent. However, the power losses associated with compressing, mixing, and heating by which diluent result in a lower power island efficiency for the IGCC case.

This highlights some of the advantages of the SOFC system. Instead of purchasing a large >800 MW gas turbine, a few smaller (<100 MW) turbines can be purchased without the high-temperature complications from combustion or dilution needs, reducing the risk of operation. Second, the SOFCs, as a relatively new technology, will have a larger cost per kW of power output than the gas turbine. However, the SOFCs need to provide only 563 MW of power, shifting the power burden to technologies that are more mature and less expensive. On the whole, this will reduce the impact of the capital cost and scale-up hurdles that presently stand in the way of industrial-scale implementation of SOFCs. Furthermore, the SOFC stacks consist of thousands of fuel cells, which can be wired to any degree of segmentation with no moving parts. A failure in an individual cell or even an entire module need not completely shut down the plant, since the remaining fuel cells can continue their function. For the IGCC plant, on the other hand, the risk of shutdown of the primary gas turbine raises reliability concerns.

Water consumption

Several different cooling systems can be used for the requirements of the HRSG and other units. With once-through cooling, water from a natural reservoir is passed through the cooling system and returned to the environment somewhat warmer than when it was withdrawn. This requires a relatively negligible auxiliary power load. If recirculating cooling towers are used instead, significantly less water can be withdrawn, but at the expense of 0.8–1.5% drop in power output and increased water losses due to evaporation. Similarly, a dry cooling system (using air instead of water) can provide cooling at a 4–9% drop in power output, but consumes no water for cooling purposes.[52]

Because water withdrawal is an issue of increasing concern, particularly for coal power plants,[53] few new plants are constructed with once-through cooling and instead use recirculatory cooling towers. An average of 0.6 L of fresh water is consumed per MJ of electricity produced by fossil fuel power plants in the western US (94% of these are pulverized coal).[54] Using cooling towers, the more modern IGCC plants can reduce this water consumption by about 30%. Although the losses in IGCC are lower, a significant amount of water is lost to the atmosphere through the flue. Some of the water lost in the flue is generated by gasification and combustion. The remaining water lost in the flue originated as water fed to the gasifier or as steam to the WGS reactors. Only about half of this input can be provided by recycle from downstream processes, such as the Claus process.

For the SOFC-based process, the water that would otherwise be lost to the atmosphere is captured as a high purity byproduct of CO_2/H_2O separation. Because of the water generated by gasification and oxidation, there is enough water available to supply all of the upstream water needs (via streams 8.1, 8.2, and 9.3). Thus, a surplus is generated (stream 8.6). Along with the waste water from the Claus process, this surplus water can be used in recirculating cooling towers to reduce the consumption from a natural source. If a dry cooling system were used, the surplus water can be treated and used for municipal or other

Table 4. Power, Efficiency, and Water Statistics for a Variety of Power Plant Combinations Using 227 tonne/h of Illinois #6 Bituminous Coal

		Power Out. (MW)		Electrical Efficiency		Water Use (Bln L/yr)	
		No	Yes	No	Yes	No	Yes
Type	Cooling strategy	CO_2 Cap	CO_2 Cap	CO_2 Cap	CO_2 Cap	CO_2 Cap	CO_2 Cap
PC	Once-through cooling	630	568	36.8%	24.9%	10.8*	
PC	Wet cooling towers	623	562	36.4%	24.7%		
PC	Dry cooling towers (air cooled)	585	528	34.2%	23.2%		
IGCC	Once-through cooling	654	592	38.2%	34.6%	6.8	6.8
IGCC	Wet cooling towers	647	586	37.8%	34.3%	7.6	7.6
IGCC	Dry cooling towers (air cooled)	608	551	35.5%	32.2%	1.6	1.6
SOFC	Once-through cooling	780	766	45.6%	44.8%	7.1	4.6
SOFC	Wet cooling towers	772	758	45.1%	44.3%	8.2	5.7
SOFC	Dry cooling towers (air cooled)	725	712	42.4%	41.6%	1.5	−1.0

*Water consumption for PC is taken as the average value for existing plants in the US West—about 50% of these use once-through cooling, and essentially none use CO_2 capture.

purposes, due to its high purity. This is particularly advantageous in water-stressed regions of the world.

The approximate water consumption for a variety of plant configurations can be found in Table 4 and Figure 5. In these figures, the PC results (Cases 9 and 10) and the IGCC results (Cases 1 and 2) are based on the NETL report.[6] Energy penalties for wet and dry cooling towers are taken as 1% and 7% from the base case (once-through), respectively.

Other emissions and pipeline

As an additional benefit of the SOFC process, H_2S compounds not captured by absorption are sequestered as well. This reduces total SO_2 emissions by 411 tonne/year compared with the IGCC plant. However, further attempts to redirect some of the sulfur to the CO_2 pipeline are inadvisable, because the SOFCs and the CO_2 pipeline can only tolerate a small increase in the H_2S concentration.

The impurities in the CO_2 stream captured by the SOFC based plant are shown in Table 5, along with pipeline specifications from several organizations.[50] The CO_2 stream captured from the SOFC plant meets these pipeline specifications, except for the Weyburn pipeline, which permits higher H_2S and hydrocarbon concentrations at the expense of water and inert gas tolerance. The oxygen concentration, though low in the steady-state solution, is heavily influenced by the quality of control of the O_2 fed to the oxidation reactor.

Comparison with other processes

Several other SOFC-based power generation systems have been proposed, although none have yet been demonstrated on the industrial scale. Many proposed processes do not include a water gas shift reaction step.[8,14,31,55–65] These processes specify either the use of unshifted (CO rich) syngas as the fuel or the use of a different type of gasifier to produce a high methane gas fuel instead of syngas. In the case of syngas, the fuel cell is susceptible to carbon deposition according to reaction (9), as discussed in the ''Syngas shifting'' section. If the SOFC fuel contains methane then CO is formed in the SOFC anode through the endothermic steam reforming reaction:

$$CH_4 + H_2O \leftrightarrow CO + 3H_2 \tag{17}$$

and through the water gas shift reaction (8). This ''internal reforming'' mechanism absorbs some of the heat released by electrochemical oxidation of the H_2 and CO, and thus reduces the need for interstage cooling between SOFC modules. However, the propensity for coking remains via reaction (9). Furthermore, methane cracking also occurs:

$$CH_4(g) \leftrightarrow 2H_2(g) + C(s) \tag{18}$$

which produces helpful hydrogen gas but problematic carbon solids as well. Although current research in anode materials aims to tackle the carbon deposition problem, we believe that large scale commercialization will be more likely if the risk of deposition is mitigated by avoiding coking conditions altogether.

Other proposed SOFC-based processes do include a water gas shift reaction step but place the CO_2 separation step upstream of the SOFC stage.[11–17] This requires the use of a solvent such as Selexol, for an absorption process in addition to the absorption process used for H_2S removal. However,

Table 5. Various CO_2 Pipeline Specifications[50] and Corresponding Concentrations Achieved in the Proposed SOFC-Based Process

	Kinder Morgan	Weyburn	Sleipner	Dynamis	SOFC Plant
H_2O	<690 ppm	<20 ppm	<Saturated	<500 ppm	501 ppm
CO_2	>95%	>96%	>93–96%	>95.5%	96.6%
H_2S	10–200 ppm	<0.9%	<150 ppm	<200 ppm	58 ppm
CO	–	<0.1%	–	<0.2%	1 ppm
C_xH_y	<5%	<2.3%	<0.5–2.0%	<2%	17 ppm
H_2, N_2, Ar	<4%	<300 ppm	<3–5%	<4%	3.3%
O_2	<10 ppm	<50 ppm	–	–	6 ppm

these processes carry a large power and capital cost penalty for this technique, as discussed in the "CO_2 capture consequences" section.

A variety of concepts have been considered which propose the use of H_2 or CO_2 membranes to remove the desired components from syngas or fuel exhausts, and a full comparison is outside the scope of this work. However, current membrane technology is generally unable to achieve adequate recoveries and purities necessary to facilitate sufficient CO_2 capture.[66] Other obstacles include the high capital cost of membranes,[67] power losses due to large pressure drops, and the general lack of availability of the rare or precious metals sometimes necessary to construct membranes for use on a world scale.

One attractive characteristic of the proposed process is that it can be constructed without CO_2 capture capability and remain "capture ready." That is, the fuel exhaust, after heat recovery and expansion, can be vented to the atmosphere in the flue since currently regulated pollutants are already removed upstream. The CO_2 capture and compression steps can be added at a later date by diverting the flue to flash cascade and compression systems at little penalty for retrofit beyond the cost of that equipment. This is currently not cost feasible for traditional coal plants. Although CO_2 regulations in the United States are expected, rapidly developing countries such as China and India are less likely to enact carbon restrictions. Corporations seeking to invest in new power generation stations in those regions can reduce their initial risk by building the capture-ready version of the plant.

Levelized cost of electricity

Estimates for the levelized cost of electricity (LCOE) have been computed for a variety of process configurations and cap-and-trade scenarios. For purposes of comparison, capital and operating costs for PC without CCS, PC with CCS, IGCC without CCS, and IGCC with CCS were taken from Cases 9, 10, 1, and 2 of the NETL report,[6] respectively. Specifically, these include the costs for coal handling, water handling (including cooling towers), air separation, gasification, syngas scrubbers, the Claus plant, water gas shift units (and catalysts), CO_2 compression, gas turbines, air compressors, steam turbines, condensers, steam generators, the stack, electrical hardware (transformers, etc.), control systems, facilities, structures, catalysts, solvents, labor, maintenance, waste disposal, water, fuel, CO_2 transport and storage, and miscellaneous pumps and accessories.

Costs for the 1-Stage and 2-Stage Selexol processes estimated by the NETL were replaced with rigorous in-house calculations (Bashadi S, MIT Energy Initiative, personal communication) for all IGCC and SOFC applications with carbon capture. For SOFC processes, equipment costs were computed in-house using Aspen Icarus 2006.5 software for units which were not contained in that report. For example, the oxidation reactor in the SOFC cases was scaled to achieve a superficial velocity of 1.0 m/s with an aspect ratio of 1.79, to achieve near 100% oxidation of H_2 at high temperature in a catalytic bed.[68] Also, the cost of a fuel cell unit is uncertain, and so was taken as a parameter (note that \$490/kW is the US DOE target price for 2010[69]). Additionally, the condenser, the flash drums, and the recycle compressors in the CO_2/H_2O removal section of the SOFC cases were modeled with Aspen Icarus, as well as the cathode exhaust expander, SOFC fuel expander, oxidation unit oxygen compressor, and cathode air compressors of the SOFC power island section. All prices taken from the NETL report or predicted by Aspen Icarus include the direct and indirect costs equipment, materials, installation labor, wiring, and contingencies. When necessary, unit costs were scaled using the six-tenths rule:

$$C_{\text{actual}} = C_{\text{quoted}} \left(\frac{F_{\text{actual}}}{F_{\text{quoted}}} \right)^{0.6}, \tag{19}$$

Where C_{quoted} and F_{quoted} are the quoted cost and scaling factor and C_{actual} and F_{actual} are the new cost and scaling factors, respectively. Example scaling factors used in this analysis are the CO_2 flow rate for a CO_2 compressor, the cooling duty for a condenser, or the amount of power handled by the electrical transformers.

All plants were then scaled to the same rate of coal feed, operating at 80% of capacity (about 182 ton/h). The LCOE was computed using:

$$\text{LCOE} = \frac{\sum_{y=1}^{N} (C_y + A_y)(1-d)^{-y}}{E \sum_{y=1}^{N} (1+d)^{-y}}, \tag{20}$$

where d is the assumed discount rate of 10%, N is the 20-year lifetime outlook, E is the total electricity produced per year, C_y is the capital expense in year y, and A_y is the total operating costs of year y.[70] It is assumed that all capital expenses are paid in the first year ($C_y = 0$ for $y > 1$), and that the annual operating costs inflate at a rate of $i = 2.8\%$ per year according to:

$$A_y = A_1(1+i)^{y-1} + P_y, \tag{21}$$

Table 6. Cost Comparison of Several Coal-Based Power Generation Processes in \$1Q2007

	SOFC at \$500/kW	SOFC at \$1000/kW	IGCC with no CCS	IGCC with CCS	PC with no CCS	PC with CCS
CO_2 sequestered (tonne/year)	3,639,074	3,639,074	–	3,426,154	–	3,396,186
CO_2 emitted (kg/MWh)	0	0	796	53	855	126
Total capital cost (\$1000s)	\$1,462,411	\$1,743,911	\$1,176,138	\$1,300,422	\$923,901	\$1,364,421
Total operating cost (\$1000s/year)	\$128,057	\$128,057	\$126,696	\$133,125	\$110,531	\$117,274
Electricity generated (MWh/year)	5,368,026	5,368,026	4,585,336	4,149,611	4,409,928	2,980,670
HHV thermal efficiency	44.8%	44.8%	38.2%	34.6%	36.8%	24.9%
LCOE (¢/kWh)	5.79	6.35	6.08	7.60	5.27	9.64

Both SOFC options include 100% CCS. Plants operate at 80% of capacity.

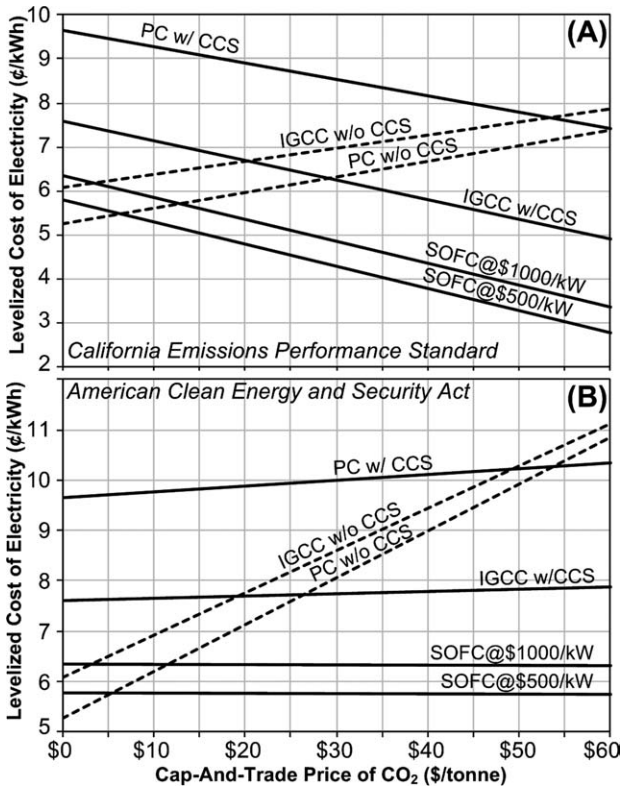

Figure 7. The effects of cap-and-trade legislation on various coal-based power plants.

(A) A fixed-cap approach according to the California Emissions Performance Standard. (B) Based on the allocation limits in The American Clean Energy and Security Act of 2009 (ACESA).

where P_y is the expense of carbon credits in year y, when incorporated as described in the next section.

A summary of the results can be found in Table 6, and an itemized list of capital and operating costs can be found in the Supporting Information included in the online version of this journal. It should be noted that though the capital costs were rigorously estimated, the results of this analysis are more useful as a comparison between designs rather than an accurate assessment of the actual costs. In particular, the parameters used in the finance model will also impact these results. For example, if the discount rate were increased by 4 pp (from $d = 10$–14%), the resulting LCOE values for the six cases increase by ~8–10%. Conversely, decreasing the discount rate to 6% lowers the LCOE by 8–10%. Similarly, if the annual inflation rate i were increased or decreased by 1 pp, the LCOEs increase or decrease by about 3–4%, respectively. Other financing considerations were not taken into account, such as taking out a loan to pay the capital costs over many years, maintaining cash reserves, working capital, depreciation, taxes, and various business expenses, which are outside the scope of this study. Together, these will increase the predicted LCOEs of each case, but the differences between them will remain relatively unchanged.

Cap-and-trade scenarios

The effects of potential cap-and-trade systems on the bottom line LCOE were also considered. First, a fixed-cap approach is taken, where the CO_2 emissions limit is fixed throughout the lifetime of the plant. If emissions exceed that limit, then carbon credits must be purchased to offset that difference. Conversely, if emissions are below the limit, the difference is sold. Based on the average market price of CO_2 for the plant lifetime, the LCOE is recomputed. Figure 7A shows the LCOE (for the same six scenarios shown in Table 6) as a function of the average lifetime market price of CO_2, using an emissions cap of 500 kg/MWh. This is approximately the average emission rate of a natural gas combined cycle plant and is the current limit under the California Emission Performance Standard. Note that 150 kg/MWh has been suggested as a potential future standard for California.[71]

Recently, the American Clean Energy and Security Act of 2009 (ACESA) was passed in the US House of Representatives, which includes a cap-and-trade system based on a schedule of gradually decreasing emissions allowances.[72] The bill specifies the total amount of nationwide CO_2 emission allowances (in total tons of CO_2 emitted) for each year from 2012 to 2050, decreasing from 2005 levels, but it is not clear how or on what basis those allowances would be available for purchase by each sector (electricity production, concrete manufacturing, etc.) or to individual contributors. In 2005, coal-derived electricity generated 1964 million tonnes of CO_2 emissions or about 32.6% of all US emissions.[73] Therefore, it is assumed that 32.6% of all future allowances would be available to the coal-derived electricity sector. Also in 2005, this sector produced ~2013 TWh of electricity,[74] and is projected to grow at an average rate of 0.7% per year.[75] This gives an average of 976 kg/MWh emitted in 2005 (for all types of coal), which is consistent with the results for PC in Table 6. Using these numbers, the projected allowances available for purchase by for coal-derived electricity plants are computed in Table 7. It is assumed that offsets are purchased to cover any emissions above the purchased allowances in a given year at 1.5 times the market rate of a CO_2 allowance. Additionally, ACESA provides a small amount of credits to be given free to plants constructed before 2020 with at least 50% CO_2 capture. Although it is uncertain how these will be distributed, we

Table 7. Projected CO_2 Emissions Allowances for Coal-Derived Electricity Plants under the American Clean Energy and Security Act of 2009

Year	2012	2013	2014	2015	2016	2017	2018	2019	2020	2021
Allowances avail. (kg/MWh)	713	695	775	755	821	800	778	757	737	709
Free credits for CCS-enabled plants (kg/MWh)	0	0	5	5	6	7	7	8	8	9
Year	2022	2023	2024	2025	2026	2027	2028	2029	2030	2031
Allowances avail. (kg/MWh)	683	656	630	604	579	554	529	504	480	460
Free credits for CCS-enabled plants (kg/MWh)	10	11	12	14	15	16	18	20	22	24

compute a schedule shown in Table 7 of the amount of free credits provided to CCS-enabled plants. This is calculated by using the schedule of freely given allowances in §782 of the bill and assuming that 1000 MW of power are produced from CCS-enabled plants with an average of 50% capture, and that this increases at a rate of 10% per year. It is assumed that these credits are sold at the market rate if they are in excess of emissions.

Following the ACESA schedule, the LCOE is computed for each plant configuration as a function of the lifetime average price of a CO_2 emission credit and shown in Figure 7B. Additionally, this analysis does not consider CO_2 emission equivalents (such as methane, nitrous oxides, etc).

In general, Figure 7 indicates that for either cap-and-trade system, the SOFC plant (even at \$1000/kW) is consistently more attractive than any of the CCS-enabled technologies considered, having an LCOE of 0.8–1.6¢/kWh lower than IGCC with CCS. Despite this, there is still not enough financial incentive for a private investor to choose SOFC with CCS (or any CCS-enabled process) over traditional PC without legislatively induced incentives. However, under either policy, even a weak set of emissions limits will make SOFC the most attractive option if the carbon credit price is above only \$5–\$12/tonne—A small number considering the lowest recent market price seen on the European Climate Exchange was about \$10.24/tonne in February 2009, at the worst of the economic downturn when allowances were plentiful due to reduced electricity output. In the ACESA framework, the amount of free credits has a negligible impact on the LCOE for any of the CCS cases, as shown by the very slight decrease in the LCOE of SOFC w/ CCS with increasing carbon price. However, in the California system, with many free credits provided initially, CCS is heavily incentivized because the LCOE can be greatly reduced as the carbon price increases.

Conclusions

By combining coal gasification with solid oxide fuel cells for power generation, significant efficiency advantages over turbine-based systems are achieved. In particular, the use of SOFCs with unmixed anode and cathode exhausts makes the process inherently CO_2 capture friendly, where simple CO_2 capture systems can be constructed without negatively affecting other areas of the flowsheet. This is a stark contrast to both traditional and modern alternatives to coal-derived power generation with CO_2 capture, where most solutions induce a large parasitic power load somewhere in the process. As a result, the proposed process enjoys a very high efficiency, on par with most other concepts using SOFCs. Furthermore, the levelized cost of electricity for the SOFC-based process is lower for any of the other carbon-capture-enabled processes considered. This process, to our knowledge, appears to be the first to avoid the carbon deposition issues that threaten long-term viability of the fuel cells and achieve zero atmospheric emissions.

Acknowledgments

The authors thank Randall Field (MIT), Di-Jia Liu (Argonne), and the engineers at BP for their helpful insights. This project was conducted as a part of the BP-MIT Conversion research program.

Notation

ACESA = the American clean energy and security act of 2009
ASU = air separation unit
CCS = carbon capture and sequestration
HHV = higher heating value
HRSG = heat recovery and steam generation
IGCC = integrated gasification combined cycle
LCOE = levelized cost of electricity
PC = pulverized coal
pp = percentage point
PR-BM = Peng Robinson equation of state with the Boston-Mathias modification
PSRK = predictive Soave-Redlich-Kwong equation of state
SOFC = solid oxide fuel cell
WGS = water gas shift
W_{module} = the power output of a fuel cell module, for DC or AC
ΔH = enthalpy change
ΔS = entropy change
η_{module} = the overall efficiency of a fuel cell module
η_{act} = the ratio of the actual voltage achieved to the ideal voltage

Literature Cited

1. Minchener AJ, McMullan JT. Strategy for sustainable power generation from fossil fuels. *J Energy Inst*. 2008;81:38–44.
2. Blasing TJ, Broniak CT, Marland G. The annual cycle of fossil-fuel carbon dioxide emissions in the United States. *Tellus B Chem Phys Meteorol*. 2005;57B:107–115.
3. Highes S. Energy secretary backs clean-coal investments. *Wall St J*. April 7, 2009.
4. Herzog HJ, Golomb D. Carbon capture and storage from fossil fuel use. In: Cleveland CJ, editor. *Encyclopedia of Energy*. New York: Elsevier Science, 2004:277–287.
5. NETL. *Carbon Sequestration Technology Roadmap and Program Plan*. US DOE Report, 2007.
6. Woods MC, Capicotto PJ, Haslbeck JL, Kuehn NJ, Matuszewski M, Pinkerton LL, Rutkowski MD, Schoff RL, Vaysman V. *Cost and Performance Baseline for Fossil Energy Plants. Volume 1: Bituminous Coal and Natural Gas to Electricity Final Report, DOE/NETL-2007/1281*. Revision 1, August, 2007.
7. Duan L, Lin R, Deng S, Jin H, Cai R. A novel IGCC system with steam injected H_2/O_2 cycle and CO_2 recovery. *Energy Convers Manage*. 2004;45:797–809.
8. Gray D, Salerno S, Tomlinson G. *Current and Future IGCC Technologies: Bituminous Coal to Power*. Mitretek Technical Report MTR-2004–05, 2004.
9. Shelly S. Oxygen and nitrogen: onward and upward. *Chem Eng Prog*. 2009;105:1.
10. Li F, Fan LS. Clean coal conversion processes—progress and challenges. *Energy Environ Sci*. 2008;1:248–267.
11. Balan C, Smith DP. *Integrated Power Plant and System and Method Incorporating the Same*. US Patent 2006/0003207 A1, 2006.
12. Doyon J, Ghezel-Ayagh H, Walzak J, Junker ST, Patel D, Adriani A, Huang P, Stauffer D, Vaysman V, White JS, Borglum B, Tang E, Petri R, Sishtla C. SECA coalbased multi-MW SOFC power plant development. In: *Fuel Cell Seminar and Exposition*, San Antonio, TX, October 15–19, 2007.
13. Ghezel-Ayagh H. Solid oxide fuel cell program at fuelcell energy Inc., In: *9th Annual 2008 SECA Workshop*, Pittsburgh, PA, August 5–7, 2008.
14. Grol E, Keairns D, Newby D. Integrated gasification fuel cell (IGFC) system studies, In: *9th Annual 2008 SECA Workshop*, Pittsburgh, PA, August 5–7, 2008.
15. Keefer BG, Babicki ML, Kirby MH. *Enhanced Solid Oxide Fuel Cell Systems*. US Patent 2008/0090113 A1, 2008.
16. Krüger M, Wörner A, Müller-Steinhagen H. Solid oxide fuel cell (SOFC) hybrid power plant with integrated coal gasification: process variations and possible ways to separate carbon dioxide. *Chem Ing Tech*. 2007;79:1323.
17. Vora SD. SECA program review. In: *9th Annual 2008 SECA Workshop*, Pittsburgh, PA, August 5–7, 2008.
18. Pierre J. Siemens energy. In: *10th Annual Solid State Energy Conversion Alliance (SECA) Workshop*, Pittsburgh, PA, July 14–16, 2009.

19. Ghezel-Ayagh H. Solid oxide fuel cell program at FuelCellEnergy Inc. In: *10th Annual Solid State Energy Conversion Alliance (SECA) Workshop*, Pittsburgh, PA, July 14–16, 2009.
20. Surdoval WA. Clean economic energy in a carbon challenged world. In: *10th Annual Solid State Energy Conversion Alliance (SECA) Workshop*, Pittsburgh, PA, July 14–16, 2009.
21. Aspen Technology, Inc. *Aspen Plus User Guide, Version 2006.5, Software Documentation*. Aspen Technology, Inc., Burlington, MA, 2006.
22. Valtz A, Chapoy A, Coquelet C, Paricaud P, Richon D. Vapour-liquid equilibria in the carbon dioxide-water system, measurement and modeling from 278.2 to 318.2 K. *Fluid Phase Equilib*. 2004;226:333–344.
23. Bamberger A, Sieder G, Maurer G. High-pressure (vapor + liquid) equilibrium in binary mixtures of (carbon dioxide + water or acetic acid) at temperatures from 313 to 353 K. *J Supercrit Fluids*. 2000;17:97–110.
24. Xu N, Dong J, Wang Y, Shi J. High pressure vapor liquid equilibria at 293 K for systems containing nitrogen, methane, and carbon dioxide. *Fluid Phase Equilib*. 1992;81:175–186.
25. Carrero-Mantilla J, Llano-Restrepo M. Vapor-liquid equilibria of the binary mixtures nitrogen + methane, nitrogen + ethane and nitrogen + carbon dioxide, and the ternary mixture nitrogen + methane + ethane from Gibbs-ensemble molecular simulation. *Fluid Phase Equilib*. 2003;208:155–169.
26. Yucelen B, Kidnay AJ. Vapor-liquid equilibria in the nitrogen + carbon dioxide + propane system from 240 to 330 K at pressures to 15 MPa. *J Chem Eng Data*. 1999;44:926–931.
27. Pope JE. *Rules of Thumb for Mechanical Engineers*. Houston: Gulf Professional Publishing, 1997:117.
28. Shin Nippon Machinery. *C Type Condensing Multistage Steam Turbine, Online Product Specifications*. Available at: http://www.snm.co.jp/products/turbines/fukusui_01.html, accessed on Dec., 2009.
29. Watkinson AP, Lucas JP, Lim CJ. A prediction of performance of commercial coal gasifiers. *Fuel*. 1991;70:519–527.
30. Kuramochi T, Wu H, Ramírez A, Faaij A, Turkenburg W. Techno-economic prospects for CO_2 capture from a solid oxide fuel cell—Combined heat and power plant. Preliminary results. *Energy Proc*. 2009;1:3843–3850.
31. Lobachyov K, Richter JH. Combined cycle gas turbine power plant with coal gasification and solid oxide fuel cell. *J Energy Resour Technol*. 1996;118:285–292.
32. Sasaki K, Susuki J, Iyoshi A, Uchimura M, Imamura N, Kusaba H, Teraoka Y, Fuchino H, Tsujimoto K, Uchida Y, Jingo N. H_2S poisoning of solid oxide fuel cells. *J Electrochem Soc*. 2006;153:A2023–A2029.
33. Trembly JP, Marquez AI, Ohrn TR, Bayless DJ. Effects of coal syngas and H_2S on the performance of solid oxide fuel cells: single-cell tests. *J Power Sources*. 2006;158:267–273.
34. Haga K, Adachi S, Shiratori Y, Itoh K, Sasaki K. Poisoning of SOFC anodes by various fuel impurities. *Solid State Ionics*. 2008;179:1427–1431.
35. EG&G Technical Services, Inc. *Fuel Cell Handbook*, 7th ed. DOE/NETL, Morgantown, WV, 2004;7.28–7.29.
36. Acosta A, Aineto M, Iglesias I, Romero M, Rincón JM. Physicochemical characterization of slag waste coming from GICC thermal power plant. *Mater Lett*. 2001;50:246–250.
37. Trembly JP, Gemmen RS, Bayless DJ. The effect of coal syngas containing HCl on the performance of solid oxide fuel cells: investigations into the effect of operational temperature and HCl concentration. *J Power Sources*. 2007;169:347–354.
38. Malkow T. SOFC in brief. In: Bove R, Ubertini S, editors. *Modeling Solid Oxide Fuel Cells*. Berlin: Springer, 2008:3–12.
39. Marquez AI, Ohrn TR, Trembly JP, Ingram DC, Bayless DJ. Effects of coal syngas and H_2S on the performance of solid oxide fuel cells: part 2. Stack tests. *J Power Sources*. 2007;164:659–667.
40. Kee RJ, Zhu H, Sukeshini AM, Jackson GS. Solid oxide fuel cells: operating principles, current challenges, and the role of syngas. *Combust Sci Technol*. 2008;180:1207–1244.
41. Lim T-H, Song R-H, Shin D-R, Yang J-I, Jung H, Vinke IC, Yang S-S. Operating characteristics of a 5kW class anode-supported planar SOFC stack for a fuel cell/gas turbine hybrid system. *Int J Hydrogen Energy*. 2008;33:1076–1083.
42. Adams TA, Barton PI. A dynamic, two-dimensional heterogeneous model for water gas shift reactors. *Int J Hydrogen Energy*. 2009;34:8877–8891.
43. Chen W-H, Jheng J-G. Characterization of water gas shift reaction in association with carbon dioxide sequestration. *J Power Sources*. 2007;172:368–375.
44. Süd-Chemie. *C25-1-02 Product Bulletin. Corporate Literature*, undated.
45. Rao A, Akshay V, Cortez DH. Optimization of the shift conversion unit in a gasification plant. In: *Gasification Technologies Council Annual Meeting*, Washington DC, October, 2006.
46. Grol E, Yang W-C. *Evaluation of Alternate Water Gas Shift Configurations for IGCC Systems, DOE/NETL-401-080509*. August 5, 2009.
47. Ohtsuka Y, Tsubouchi N, Kikuchi T, Hashimoto H. Recent progress in Japan on hot gas cleanup of hydrogen chloride, hydrogen sulfide and ammonia in coal-derived fuel gas. *Powder Technol*. 2009;190:340–347.
48. Trembly JP, Gemmen RS, Bayless DJ. The effect of IGFC warm gas cleanup system conditions on the gas-solid partitioning and form of trace species in coal syngas and their interactions with SOFC anodes. *J Power Sources*. 2007;163:986–996.
49. Adams TA, Barton PI. *Systems and Methods for the Separation of Carbon Dioxide and Water*. US Patent 12/434486, 2009.
50. deVisser E, Hendriks C, Barrio M, Mølnvik MJ, de Koeijer G, Liljemark S, Gallo YL. Dynamis CO_2 quality recommendations. *Int J Greenhouse Gas Control*. 2008;2:478–484.
51. Pålsson J, Hansen JB, Christiansen N, Nielsen JU, Kristensen S. Solid oxide fuel cells—assessment of the technology from an industrial perspective, In: *Proceedings of the Risø International Energy Conference*, Denmark, May 19–21, 2003.
52. Littleton DJ, McGurl GV, Feeley TJ, Shelton WW, Parsons EL, Smith DN, Gross RW, Veil JA. *Energy Penalty Analysis of Possible Cooling Water Intake Structure Requirements on Existing Coal-Fired Power Plants*. NETL, DOE/OFE, and Argonne National Laboratory report, 2002.
53. Frazer L. Low water consumption: a new goal for coal. *Environ Health Perspect*. 2004;112:A296–A299.
54. The Energy & Hewlett Foundations. *The Last Straw: Water Use by Power Plants in the Arid West*. White paper, 2003.
55. Am O, Vik A. *Fuel Cells*. WO Patent 02/065564 A2, 2002.
56. Araiki T, Taniuchi T, Sunakawa D, Nagahama M, Onda K, Kato T. Cycle analysis of low and high H_2 utilization SOFC/gas turbine combined cycle for CO_2 recovery. *J Power Sources*. 2007;171:464–470.
57. Gaiffi S. *System and Method for Conversion of Hydrocarbon Materials*. WO Patent 2006/119118 A2, 2006.
58. Galloway TR. *Process and System for Converting Carbonaceous Feedstocks into Energy Without Greenhouse Gas Emissions*. US Patent 2007/0099038 A1, 2007.
59. Lightner G. *Production of Electricity from Fuel Cells Depending on Gasification of Carbonaceous Compounds*. US Patent 2004/0023085 A1, 2004.
60. Lisbona P, Romeo LM. Enhanced coal gasification heated by unmixed combustion integrated with an hybrid system of SOFC/GT. *Int J Hydrogen Energy*. 2008;33:5755–5767.
61. Mayer G. *Power Generation Cycle with a Fuel Cell and a Combined-Cycle Power Plant*. DE Patent 102004038435/A1, 2006.
62. Minh NQ. Coal based solid oxide fuel cell technology development. *ECS Trans*. 2007;7:45–50.
63. Rao AD, Verma A, Samuelsen GS. Engineering and economic analyses of a coal-fueled solid oxide fuel cell hybrid power plant. *Proc ASME Turbo Expo*. 2005;3:545–553.
64. Stiegel GJ, Ramezan M. Hydrogen from coal gasification: an economical pathway to a sustainable energy future. *Int J Coal Geol*. 2006;65:173–190.
65. Zhang W. *Simulation of Solid Oxide Fuel Cell Based Power Generation Processes with CO_2 Capture*. Master's Thesis, University of Waterloo, Canada, 2006.
66. Pennline HW, Luebke DR, Jones KL, Myers CR, Morsi BI, Heintz YJ, Ilconich JB. Progress in carbon dioxide capture and separation research for gasification-based power generation point sources. *Fuel Process Technol*. 2008;89:897–907.
67. Criscuoli A, Basile A, Drioli E, Loiacono O. An economic feasibility study for water gas shift membrane reactor. *J Membr Sci*. 2001;181:21–27.
68. Younis LB. Modelling of hydrogen oxidation within catalytic packed bed reactor. *J Energy Inst*. 2006;79:222–227.

69. Williams MC, Strakey JP, Surdoval WA. U.S. DOE solid oxide fuel cells: technical advances. In: *207th Meeting of the Electrochemical Society*, Quebec City, QC, Canada, May 16–18, 2005:1025.
70. Deutch JM, Lester RK. *Making Technology Work: Applications in Energy and the Environment*. New York: Cambridge University Press, 2004:58–60.
71. Wartmann S, Jaworski P, Klaus S, Beyer C. *Scenarios on the Introduction of CO_2 Emission Performance Standards for the EU Power Sector*. Ecofys Germany GmbH, Nuremberg, Germany, white paper, January, 2009.
72. Waxman HA, Markey EJ. *The American Clean Energy and Security Act of 2009*. Proposal to US House of Representatives, HR 2454, July 6, 2009.
73. Conti J, Sweetnam GE. *Emissions of Greenhouse Gases in the United States 2007, US DOE/EIA-0573 (2007)*. December, 2008.
74. Energy Information Administration. Electric Power Annual 2007, US DOE/EIA-0348 (2007). January, 2009.
75. Energy Information Administration. Annual Energy Outlook 2009 with Projections to 2030, US DOE/EIA-0383 (2009). March, 2009.

Manuscript received June 19, 2009, revision received Dec. 3, 2009, and final revision received Feb. 21, 2010.